Bulk Magnetic Order in a Two-Dimensional Ni^{1+}/Ni^{2+} (d^9/d^8) Nickelate, Isoelectronic with Superconducting Cuprates

Viktor V. Poltavets,[1,2] Konstantin A. Lokshin,[3] Andriy H. Nevidomskyy,[4] Mark Croft,[4] Trevor A. Tyson,[5] Joke Hadermann,[6] Gustaaf Van Tendeloo,[6] Takeshi Egami,[3,7,8] Gabriel Kotliar,[4] Nicholas ApRoberts-Warren,[9] Adam P. Dioguardi,[9] Nicholas J. Curro,[9] and Martha Greenblatt[1]

[1]*Department of Chemistry and Chemical Biology, Rutgers University, Piscataway, New Jersey 08854, USA*
[2]*Department of Chemistry, Michigan State University, East Lansing, Michigan 48824, USA*
[3]*Department of Materials Science and Engineering, University of Tennessee, Knoxville, Tennessee 37996, USA*
[4]*Department of Physics and Astronomy, Rutgers, The State University of New Jersey, Piscataway, New Jersey 08854, USA*
[5]*Department of Physics, New Jersey Institute of Technology, Newark, New Jersey 07102, USA*
[6]*Electron Microscopy for Materials Research (EMAT), , USAUniversity of Antwerp, B-2020, Antwerp, Belgium*
[7]*Department of Physics and Astronomy, University of Tennessee, Knoxville, Tennessee 37996, USA*
[8]*Oak Ridge National Laboratory, Oak Ridge, Tennessee 37831, USA*
[9]*Department of Physics, University of California, Davis, California 95616, USA*

(Received 16 August 2009; published 19 May 2010)

The Ni^{1+}/Ni^{2+} states of nickelates have the identical ($3d^9/3d^8$) electronic configuration as Cu^{2+}/Cu^{3+} in the high temperature superconducting cuprates, and are expected to show interesting properties. An intriguing question is whether mimicking the electronic and structural features of cuprates would also result in superconductivity in nickelates. Here we report experimental evidence for a bulklike magnetic transition in $La_4Ni_3O_8$ at 105 K. Density functional theory calculations relate the transition to a spin density wave nesting instability of the Fermi surface.

DOI: 10.1103/PhysRevLett.104.206403 PACS numbers: 71.20.Ps, 71.18.+y, 71.45.−d

Initially Bednorz and Müller focused their search for superconductivity on the La-Ni-O system with Ni in a 2 + /3+ oxidation state [1]. After the discovery of superconductivity in the cuprates [2], other transition metal oxides were investigated for superconductivity, and aside from the cobaltates no other system has been discovered to date. The nickelates, however, have the potential to exhibit physics similar to the cuprates. Theoretical studies show that only nickelates with Ni^{1+} (d^9, $S = 1/2$) in a square planar coordination can form an antiferromagnetic (AFM) insulator directly analogous to the parent (undoped) cuprates [3]. Nickelates with Ni^{1+}/Ni^{2+} are metastable and to date, there are only a few compounds known with infinite $Ni^{1+}/Ni^{2+}O_2$ planes, and little is known about their physical properties. Here we report experimental and theoretical studies which indicate that $La_4Ni_3O_8$, a two-dimensional (2D) square planar nickelate with Ni^{1+}/Ni^{2+} (Fig. 1, supplement pg. 10 and Fig. S1 [4]), is antiferromagnetic below $T_N = 105$ K. Artificially engineered heterostructures of complex oxides are of tremendous current interest, in an effort to design specific band structures and functionalities. However, heterostructures are prone to synthetic difficulties, particularly in obtaining stoichiometry and in producing atomically smooth interfaces. $La_4Ni_3O_8$ is a ''natural'' layered compound, encompassing all the properties of the recently proposed hypothetical $LaNiO_3/LaMO_3$ (M = Al, Ga) superlattice oxide with alternating conducting NiO_2 and insulating MO_2 planes and theoretical predictions of favorable conditions for high T_c superconductivity [5].

$La_4Ni_3O_8$ is a member of the so-called T'-type $Ln_{n+1}Ni_nO_{2n+2}$ (Ln = La, Nd; $n = 2$, 3, and ∞) homologous series [6,7]. The structures of the T'-type nickelates can be described by stacking of alternating $(Ln/O_2/Ln)$ fluorite-type layers with $Ln_{n-1}(NiO_2)_n$ infinite layer structural blocks [6–8] (Fig. 1). Phases with the infinite layer structure ($n = \infty$) are known both for nickelates, $LnNiO_2$ (Ln = La, Nd) [9,10], and for cuprates, $Ca_{0.84}Sr_{0.16}CuO_2$ [11], whereas the so-called double ($n = 2$) and triple ($n = 3$) layer T'-type nickelates are unique examples of such structural arrangements [6,7]. Information on the physical properties of $La_4Ni_3O_8$ is limited to a remark that it is a

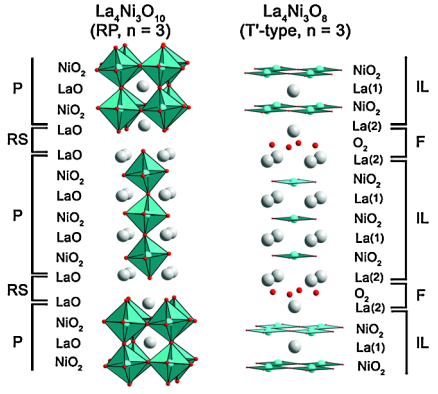

FIG. 1 (color online). Crystal structures of $La_4Ni_3O_{10}$ and $La_4Ni_3O_8$ with denoted layers and structural blocks: P, perovskite; RS, rock salt; IL, infinite layer; F, fluorite.

black semiconductor; no other physical properties have been reported previously [12].

Figure 2(a) shows the magnetization, M, of $La_4Ni_3O_8$ as a function of temperature. For large applied field ($H =$ 5 T), M exhibits a sharp drop while cooling below $T =$ 105 K [Fig. 2(a)]. This transition can be observed in magnetization measurements only at a high applied magnetic field ($H_{min} \sim 1000$ Oe), while no sign of the transition is seen in $H = 100$ Oe, even though thermodynamic measurements reveal the transition is also present in $H = 0$, as discussed below. We attribute this anomalous field dependence to the presence of a small (less than 1%) admixture of superparamagnetic Ni particles, which appears to be present in all samples. The divergence between zero-field and field-cooled curves at low temperature [<50 K; Fig. 2(a)], the non-Curie-Weiss behavior in the high temperature region, which is deduced from the nonlinear shape of the M vs H curves (Fig. S2 [4]), the nonlinear inverse magnetic susceptibility, $\chi^{-1}(T)$ (not shown) are also attributed to the small Ni impurity admixture. We found that while the value of magnetization anomaly at 105 K is reproducible for $La_4Ni_3O_8$ from different synthetic batches, the magnetization was strongly sample dependent. However, only $La_4Ni_3O_8$ was found in all samples by powder x-ray and powder neutron diffraction (NPD). High resolution transmission electron microscopy showed that the crystallites themselves are also single phase down to nanometer scale (Fig. S3 [4]).

The temperature dependence of the resistivity [Fig. 2(b)] reveals semiconducting behavior. Moreover, a clear change of slope can be seen at 105 K in Fig. 2(b). The transition temperature (~105 K) is consistent with the results of magnetic measurements, and supports the intrinsic character of the transition in $La_4Ni_3O_8$. The resistivity values measured at $H = 5$ T coincide, within experimental error, with those measured in zero field. Therefore we conclude that the transition seen at 105 K is also present at $H = 0$, but it is only detectable for H above the saturation magnetization of the admixed Ni particles, i.e., above 1000 Oe. The resistivity data below the 105 K regions are clearly insulating and can be fit to Mott's law for variable range hopping [Fig. 2(b), inset] [13]. Above the transition, the resistivity is consistent with either a bad metal, or an Anderson insulator. It should be noted that due to the metastability of $La_4Ni_3O_8$ (the sample decomposes at $T >$ 350 °C), the transport measurement could only be performed on a polycrystalline pressed pellet, where poor intergrain electrical contacts are expected. Heat capacity data for $La_4Ni_3O_8$ measured at $H = 0$ T are presented in Fig. 2(c) by circles. The lambda anomaly, peaking at 105 K, is further evidence for a bulk phase transition at this temperature. In order to estimate the entropy loss during the transition, the scaled data for the specific heat capacity of the closely related phase, $La_3Ni_2O_6$ were subtracted from those of $La_4Ni_3O_8$, and the area under the resultant peak was integrated [Fig. 2(c)]. The experimental value of ΔS_{exp} (per 1 mol of $La_4Ni_3O_8$) = 5.96 J/(mol K). The large value of the entropy loss asserts the transition to be intrinsic to $La_4Ni_3O_8$. ΔS_{exp} is close to $R \ln 2 = 5.76$ J/(mol K). In a localized model this value is close to $1/2\ R \ln 2$ per Ni^{1+}, or $1/3\ R \ln 2$ per Ni in an itinerant picture.

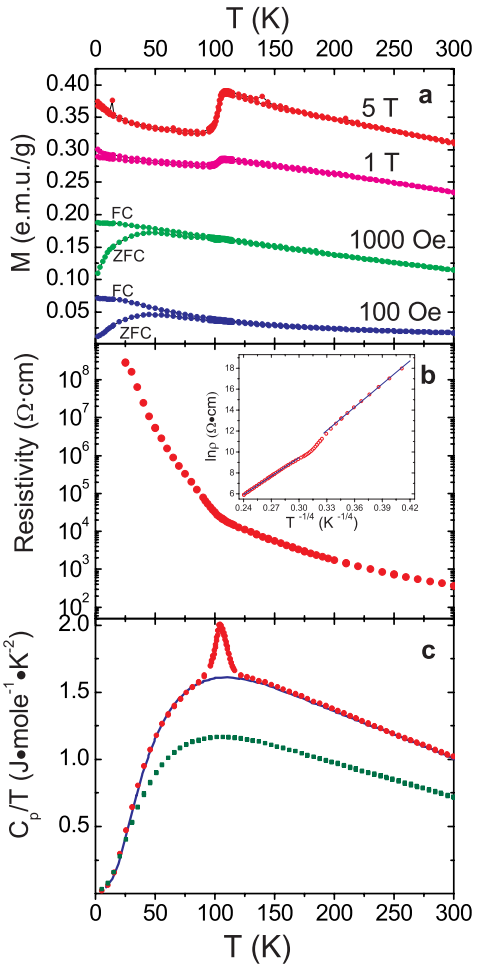

FIG. 2 (color online). Temperature dependence of selected physical properties: (a) Mass magnetization M vs temperature (T) for $La_4Ni_3O_8$ (ZFC, zero field cooling; FC, field cooling). (b) Temperature dependence of resistivity (logarithmic scale). The inset shows the natural logarithm of resistivity, $\ln(\rho)$ versus $T^{(-1/4)}$: observed data (circles) and line fits (solid lines) according to Mott's variable-range-hopping model. (c) Specific heat data of $La_4Ni_3O_8$ (circles) and $La_3Ni_2O_6$ (squares). The solid line represents the scaled specific heat of $La_3Ni_2O_6$.

Thus magnetic, resistivity and heat capacity measurements all indicate a phase transition at 105 K. The NPD pattern of $La_4Ni_3O_8$ at 15 K is identical to that at room temperature, except for a thermal contraction and expected difference in thermal factors, which indicate that this transition cannot involve a large structural displacement. Extended x-ray absorption fine structure (EXAFS) measurements support this conclusion. In addition the EXAFS

data show a sharp drop of the mean squared relative displacement (σ^2) values for the average Ni-O bond distance near ~105 K, very near the critical point, followed by a recovery at higher temperatures to the low-temperature value (Fig. S4 [4]). Recent EXAFS measurements [14] showed the same behavior of σ^2 for in-plane bonds at the spin density wave (SDW) ordering temperature in $Ca_3Co_4O_9$, a 2D magnetic oxide [15].

To probe the spin dynamics and internal hyperfine fields associated with the phase transition, we investigated the ^{139}La nuclear magnetic resonance (NMR; $I = 7/2$) in an aligned powder sample. We identify two sites with electric field gradients (EFGs) of 1.35(5) MHz and ~20(10) kHz, and assign these to La(1) (between NiO_2 planes—see Fig. 1) and La(2) (in the fluorite blocks), respectively, based on EFG calculations with WIEN2K [16]. Below the phase transition, the La(1) spectrum is washed out by the presence of a broad distribution of static hyperfine fields, whereas the La(2) resonance remains visible (see Fig. S7 [4]). The powder nature of the sample coupled with the small value of the La(2) EFG (~20 kHz) renders the La(2) spectrum nearly featureless, but we can identify two subpeaks in the spectrum which develop a significant temperature dependence below 105 K (see Fig. S8 [4]). We find an internal field ~200 Oe develops at the La(2) site with a second-order mean-field-like temperature dependence. This internal field arises from the noncancellation of the transferred hyperfine fields at the La(2) site from ordered Ni moments, and is thus a direct measure of the order parameter of this system. A similar field develops at the La(1) site, but since the hyperfine fields are much larger in the La(1) case, the spectrum is broadened considerably. In Fig. 3 we show the nuclear spin lattice relaxation rate at the two sites, which clearly shows a dramatic suppression below 105 K and confirms our interpretation that this is an intrinsic phenomenon. At high temperatures, $(T_1T)^{-1}$ approaches a constant for both sites, indicative of Fermi liquid behavior. Between 250 and 105 K $(T_1T)^{-1}$ increases dramatically, revealing critical spin fluctuations associated with AFM transition [17]. Both La(1) and La(2) exhibit similar temperature dependences for $(T_1T)^{-1}$, although $(T_1T)^{-1}$ is larger for the La(1) because of the larger hyperfine coupling to the Ni moments at this site. The behavior of the La(1) and La(2) are thus analogous to the Cu and Y nuclei in $YBa_2Cu_3O_7$ [18]. Below the ordering temperature $(T_1T)^{-1}$ once again becomes independent of temperature with a reduced value. This observation confirms our density functional theory (DFT) calculations that only a portion of the density of states at the Fermi level is gapped out and is analogous to the observed behavior in other systems, such as URu_2Si_2 [19].

In order to gain insight on the nature of the phase transition at 105 K we have determined the electronic band structure and Fermi surface (FS) with the full potential linearized augmented plane wave method as implemented in the WIEN2K package [16] (Fig. 4). There are

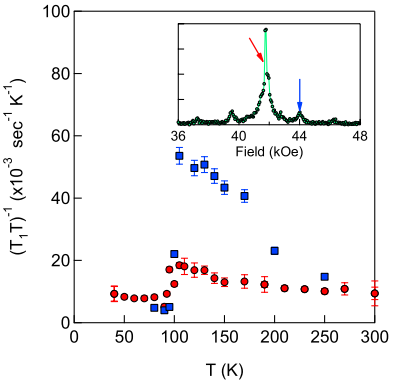

FIG. 3 (color online). The nuclear spin lattice relaxation rate of the ^{139}La versus temperature, measured at the 3/2–5/2 satellite of the La(1) (squares) and at the main line [La(1) and La(2), circles]. Inset: ^{139}La NMR spectrum in an aligned powder sample at 200 K at fixed frequency of 25.1 MHz, revealing both the axially symmetric La(1) and La(2). The arrows indicate the fields where the T_1 data were obtained.

three FS's with strong 2D character. The sheet centered at the Γ point has a square shape that could support a charge (CDW) or spin density wave (SDW) instability close to the nesting wave vector of $Q = [1/3, 1/3, L]$. FS nesting resulting in CDW or SDW transitions was shown earlier for many low-dimensional transitional metal oxides [20]. In particular, incommensurate SDW instabilities are universal for La_2CuO_4-based superconductors [21]. The absence of any change in the NPD pattern through the transition (i.e., no extra peaks, and no change in symmetry) excludes the possibility that the transition at 105 K is due to formation of a CDW state (Fig. S5 and Table S1 [4]). However, a SDW state usually results in extra magnetic peaks that should be observable by neutron scattering. The absence of magnetic peaks in the low-temperature NPD pattern suggests that the system may not be fully three-dimensionally ordered. The FS shown in Fig. 4 indicates a very strong 2D character of the electronic structure. The structure of this compound is composed of three NiO_2 layers separated by a $La/O_2/La$ layer (Fig. 1). Even though the magnetic interactions within the trilayers could

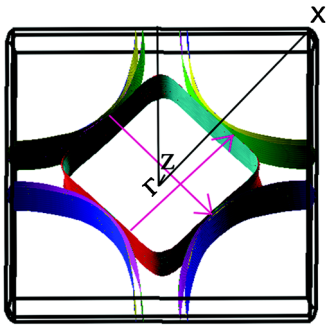

FIG. 4 (color online). Fermi surface of $La_4Ni_3O_8$ in reciprocal space with nesting vectors (arrows).

be significant, the interaction between different trilayers must be very weak. In addition, the Ni position is shifted by [1/2, 1/2] across the La/O_2/La layer, frustrating the antiferromagnetic order. Consequently there is a strong possibility that the ordering at 105 K occurs only within the trilayers. The magnetic ordering peaks will then be broad along L (c^* axis), making the detection by powder diffraction extremely difficult.

Additional DFT (LDA and LDA + U [22]) calculations have been carried out to determine the spin configuration of the ground state and the electronic structure of the material (calculation details are available in the supplementary information [4]). We find that the proposed SDW state with ordering wave vector $Q = [1/3, 1/3, 0]$ has a lower ground state energy than the paramagnetic state, confirming our previous conclusions (see supplementary information [4] for details). The Hubbard on-site interaction for Ni d-electrons, $U = 4.3$ eV, was determined by constrained DFT calculations; the U value characterizes $La_4Ni_3O_8$ as a material with intermediate electron correlations. The value of U in this nickelate is considerably smaller than in the cuprates (9–11 eV) [23] and notably larger than in the iron-pnictide superconductor $LaFeAsO_{1-x}F_x$ (1.5 eV) [24].

According to our DFT calculations within the LDA + U method, $La_4Ni_3O_8$ remains metallic. Also due to the highly anisotropic crystal structure of $La_4Ni_3O_8$ (Fig. 1) and the Fermi surface (Fig. 4), large differences in ab plane and in c direction conductivity can be expected, i.e., metallic conductivity in the infinite $Ni^{1+/2+}O_2$ planes, while semiconducting or insulating behavior perpendicular to those planes. Evidently, the semiconducting property is dominant [Fig. 2(b)] due to poor percolation in the NiO_2 planes of the poorly compacted polycrystalline sample.

To summarize, a magnetic transition at 105 K was established for $La_4Ni_3O_8$ by magnetization, resistivity, specific heat, NPD, EXAFS, and ^{139}La NMR methods. The absence of a structural transition and minute c/a ratio changes between 15 and 300 K argue against CDW or Ni^{2+} (d^8) high-spin to low-spin transitions. Thus the spin ordering or fluctuations are apparently of an AFM type. This is supported by the DFT calculations, which relate the transition to a SDW nesting instability of the FS with ordering wave vector $Q = [1/3, 1/3, L]$ with $L \approx 0$. We note that $(T_1T)^{-1}$ begins to increase at temperatures on the order of $3T_N$, which strongly suggests that the spin fluctuations are 2D, confined to the NiO_2 trilayer, and points to the presence of a smaller interlayer coupling as the origin of the long-range magnetic order. Furthermore, this strong temperature dependence of $(T_1T)^{-1}$ is similar to that observed in several unconventional superconductors, and suggests that $La_4Ni_3O_8$ may become superconducting upon appropriate doping. Once again synthetic solid state chemistry led to the realization of a bulk natural layered mixed-valent nickelate, similar to the theoretically predicted high T_c superconducting artificial heterostructure, $LaNiO_3/LaAlO_3$ [5].

This work was supported by NSF DMR-0541911 (V. V. P., M. G.); NSF DMR-0906943 (G. K.); DOE DE-FG02-99ER45790 (A. H. N.); DOE-BES DE-FG0207ER46402 (T. A. T); DOE-BES DE-FG0208ER46528 (K. A. L., T. E.); DOE-BES DE-AC02-98CH10886 (M. C.).

[1] J. G. Bednorz and K. A. Müller, Nobel Prize in Physics in 1987, http://nobelprize.org.
[2] J. G. Bednorz and K. A. Müller, Z. Phys. B **64**, 189 (1986).
[3] V. I. Anisimov, D. Bukhvalov, and T. M. Rice, Phys. Rev. B **59**, 7901 (1999).
[4] See supplementary material at http://link.aps.org/supplemental/10.1103/PhysRevLett.104.206403 for additional details of the physical properties and theoretical calculations.
[5] J. Chaloupka and G. Khaliullin, Phys. Rev. Lett. **100**, 016404 (2008).
[6] R. Retoux, J. Rodriguez-Carvajal, and P. Lacorre, J. Solid State Chem. **140**, 307 (1998).
[7] V. V. Poltavets, K. A. Lokshin, T. Egami, and M. Greenblatt, J. Am. Chem. Soc. **128**, 9050 (2006).
[8] V. V. Poltavets, M. Greenblatt, G. H. Fecher, and C. Felser, Phys. Rev. Lett. **102**, 046405 (2009).
[9] V. V. Poltavets, K. A. Lokshin, M. Croft, T. K. Mandal, T. Egami, and M. Greenblatt, Inorg. Chem. **46**, 10 887 (2007).
[10] M. Crespin, P. Levitz, and L. Gatineau, J. Chem. Soc., Faraday Trans. **79**, 1181 (1983).
[11] T. Siegrist, S. M. Zahurak, D. W. Murphy, and R. S. Roth, Nature (London) **334**, 231 (1988).
[12] P. Lacorre, J. Solid State Chem. **97**, 495 (1992).
[13] N. F. Mott, Philos. Mag. **19**, 835 (1969).
[14] T. A. Tyson, Z. Chen, Q. Jie, Q. Li, and J. J. Tu, Phys. Rev. B **79**, 024109 (2009).
[15] J. Sugiyama, C. Xia, and T. Tani, Phys. Rev. B **67**, 104410 (2003).
[16] P. Blaha, K. Schwarz, G. K. H. Madsen, D. Kvasnicka, and J. Luitz, *WIEN2K, An Augmented Plane Wave + Local Orbitals Program for Calculating Crystal Properties* (Karlheinz Schwarz, Techn. Universität Wien, Wien, Austria, 2001).
[17] N. J. Curro *et al.*, Nature (London) **434**, 622 (2005).
[18] S. E. Barrett *et al.*, Phys. Rev. B **41**, 6283 (1990).
[19] S.-H. Baek, M. J. Graf, A. V. Balatsky, E. D. Bauer, J. C. Cooley, J. L. Smith, and N. J. Curro, arXiv:0906.3040v1.
[20] E. Canadell and M. H. Whangbo, Chem. Rev. **91**, 965 (1991).
[21] B. O. Wells *et al.*, Science **277**, 1067 (1997).
[22] V. I. Anisimov, J. Zaanen, and O. K. Andersen, Phys. Rev. B **44**, 943 (1991).
[23] M. S. Hybertsen, M. Schlüter, and N. E. Christensen, Phys. Rev. B **39**, 9028 (1989).
[24] T. Kroll *et al.*, Phys. Rev. B **78**, 220502(R) (2008).